Original Article

Golden-angle radial sparse parallel magnetic resonance imaging of rectal perfusion: utility in the diagnosis of poorly differentiated rectal cancer

Mi Zhou[1,2], Hongyun Huang[2], Yingying Fan[2], Meining Chen[3], Yuting Wang[2#], Fabao Gao[1#^]

[1]Department of Radiology, West China Hospital, Sichuan University, Chengdu, China; [2]Department of Radiology, Sichuan Provincial People's Hospital, University of Electronic Science and Technology of China, Chengdu, China; [3]Department of MR Scientific Marketing, Siemens Healthineers, Shanghai, China

Contributions: (I) Conception and design: F Gao; (II) Administrative support: H Huang; (III) Provision of study materials or patients: M Zhou, M Chen; (IV) Collection and assembly of data: Y Fan; (V) Data analysis and interpretation: Y Wang; (VI) Manuscript writing: All authors; (VII) Final approval of manuscript: All authors.

[#]These authors contributed equally to this work.

Correspondence to: Fabao Gao, PhD. Department of Radiology, West China Hospital, Sichuan University, No. 37 Guoxue Alley, Wuhou District, Chengdu 610041, China. Email: gaofabao@wchscu.cn; Yuting Wang, MD. Department of Radiology, Sichuan Provincial People's Hospital, University of Electronic Science and Technology of China, Yihuan Road No. 32, Qingyang District, Chengdu 610072, China. Email: Wangyuting_330@163.com.

Background: The objective of this retrospective investigation is to evaluate the diagnostic efficacy of a dual-parameter strategy that integrates either time-resolved angiography with stochastic trajectories (TWIST) or golden-angle radial sparse parallel (GRASP)-derived dynamic contrast agent-enhanced magnetic resonance imaging (DCE-MRI) with diffusion-weighted imaging (DWI) for the identification of poorly differentiated rectal cancer (RC). The purpose of this investigation is to contrast the aforementioned methodology with conventional single-factor assessments that rely solely on DWI, and ascertain its comparative efficacy.

Methods: This study was not registered on a clinical trial platform. Consecutive individuals diagnosed with non-mucinous rectal adenocarcinoma through endoscopy-guided biopsy between December 2020 and October 2022 were involved in our study. These patients had also undergone DCE-MRI and DWI. The perfusion metrics of influx forward volume transfer constant (Ktrans) and rate constant (Kep), along with the apparent diffusion coefficient (ADC), were quantified by a pair of investigators. The study compared the area under the curve (AUC) of the receiver operating characteristic (ROC) for both sequences to identify poorly differentiated RC. The investigation incorporated patients who fulfilled the specified criteria. The inclusion criteria for the investigation were as follows: (I) a diagnosis of RC proved through pathological examination, either via endoscopically-guided biopsy or surgical resection; (II) availability of complete MRI images; (III) absence of any prior history of neoadjuvant chemoradiotherapy during the MRI scan.

Results: Our investigation comprised a total of 179 participants. Compared to diffusion parameter alone, an integrated assessment of diffusion parameter (ADC) and perfusion parameters (Ktrans or Kep) obtained with GRASP leads to a superior diagnostic accuracy (AUC, 0.97±0.02 *vs.* 0.89±0.03, 0.97±0.02 *vs.* 0.89±0.03, P=0.005 and 0.003, respectively); however, there was no additional benefit from ADC with perfusion parameters obtained from TWIST (Ktrans or Kep) (AUC, 0.93±0.04 *vs.* 0.89±0.03, 0.93±0.03 *vs.* 0.89±0.03;

^ ORCID: 0000-0003-2257-3275.

P= 0.955 and 0.981, respectively, for the integration of ADC with Ktrans and Kep).

Conclusions: By integrating diffusion and perfusion features into a dual-parameter model, the GRASP method enhances the diagnostic efficacy of MRI in discriminating RCs with poor differentiation. Conversely, the TWIST approach did not yield the aforementioned outcome.

Keywords: Time-resolved angiography with stochastic trajectories (TWIST); golden-angle radial sparse parallel (GRASP); perfusion; apparent diffusion coefficient (ADC); rectal cancer (RC)

Submitted Nov 09, 2022. Accepted for publication Jun 09, 2023. Published online Jul 06, 2023.
doi: 10.21037/qims-22-1244
View this article at: https://dx.doi.org/10.21037/qims-22-1244

Introduction

Colorectal cancer ranks third in terms of prevalence among all types of malignancies (1,2). Several factors influence the prognosis of this disease, including lymphovascular invasion (LVI), T stage, and grade of differentiation (3-5). Definitive diagnosis of tumor type and grade of differentiation can only be made with histopathological examination following resection of the mass. The development of a non-invasive and precise approach for evaluating the severity of rectal cancer (RC) could hold significant clinical significance in directing next clinical interventions.

Magnetic resonance imaging (MRI) is known to offer enhanced soft tissue contrast in comparison to computerized tomography (CT). Furthermore, diverse MRI methodologies offer tissue classification, encompassing assessments of cell density [diffusion-weighted imaging (DWI)] and tumor vascularization [dynamic contrast-enhanced MRI (DCE-MRI)] (6-11). The association between histological grade, response to neoadjuvant chemoradiotherapy (CRT), and patient prognosis has been indicated through quantitative parameters acquired from DWI and DCE-MRI (12-14). The investigation performed by Winkel *et al.* exhibited the prospective clinical applicability of quantitative DCE-MRI and DWI in evaluating the differentiation grade of prostate carcinoma (15).

The time-resolved angiography with stochastic trajectories (TWIST) technique uses view-sharing to shorten the time of acquisition of DCE-MRI (16). View-sharing involves acquiring only a subset of k-space data for each image in a time series, and then combining these subsets to reconstruct the complete image series. Although this methodology enables expedited imaging, it concurrently heightens the susceptibility of the resultant images to motion artifacts that stem from either patient motion or bowel movement. This is because the incomplete k-space sampling during each acquisition means that the reconstructed images are more sensitive to inconsistencies or changes in the position of the imaged tissue between successive acquisitions (17). In addition to patient-related artifacts, the outcomes can be impacted by discrepancies in timing between the application of contrast agents and the capture of images.

Moreover, view-sharing techniques typically result in low spatial resolution and a compromise in temporal resolution (17,18).

The golden-angle radial sparse parallel imaging (GRASP) procedure, a quick dynamic MRI free from breathing, has been introduced as an improvement to the temporal DCE-MRI resolution (18). The proposed method enhances temporal resolution through the integration of a golden-angle, motion-insensitive, stack-of-stars acquisition technique with a compressed sensing restoration approach, rendering it appropriate for unconstrained respiratory motion DCE-MRI (17). Studies have shown GRASP perfusion's ability to offer image quality comparable to traditional DCE, with reduced motion artifacts, making it particularly beneficial in RC imaging (17,19). However, literature lacks sufficient documentation on the diagnostic efficiency of GRASP's quantitative parameters in differentiating RC grades. Additionally, most of the prior research (20-22) primarily centers around the preoperative treatment response, staging, and prognosis evaluation in RC using DWI or DCE-MRI, with only a limited number of them focusing on the diagnostic accuracy of RC differentiation grade by quantitative DCE-MRI and DWI. The current investigation suggests a novel strategy of dual-parameter that integrates either GRASP or TWIST with the conventional DWI technique. The aim is to enhance the diagnostic efficacy of RC differentiation grade, in contrast to the conventional single-parameter assessment that relies solely on DWI. The objective of this

Table 1 Parameters for TWIST and GRASP

Parameter	TWIST	GRASP
TR (ms)	3.6	3.5
TE (ms)	1.44	1.64
Slice thickness (mm)	3.6	3
Matrix	192×130	256×256
FOV (mm^2)	320×320	273×394
FA (degrees)	12	12
Temporal resolution (s)	4.88	3.45

TWIST, time-resolved angiography with interleaved stochastic trajectories; GRASP, golden-angle radial sparse parallel; TR, repetition time; TE, echo time; FOV, the field of view; FA, flip angle.

investigation is to examine the diagnostic accuracy of this proposed dual-parameter procedure, by comparing GRASP or TWIST combined with established DWI, for diagnosing poorly differentiated RC against the conventional DWI-based single-parameter assessment. The present article is presented in adherence to the STARD reporting checklist (available at https://qims.amegroups.com/article/view/10.21037/qims-22-1244/rc).

Methods

Ethical statement

The present study, which involved a retrospective analysis, received approval from the Institutional Review Board under the reference number Lun Audit (Research) No. 86 of 2021. Because of the retrospective nature of the investigation, the institutional review board waived the requirement for written informed consent. The study was conducted in accordance with the Declaration of Helsinki (as revised in 2013).

Patient inclusion

This study encompassed 293 individuals who were diagnosed with non-mucinous rectal adenocarcinoma through endoscopy-guided biopsy. The data were collected between December 2020 and October 2022 in Chengdu, Sichuan Province. The study included patients who fulfilled the specified criteria. The inclusion criteria for the investigation were as follows: (I) a diagnosis of RC verified through pathological examination, either via surgical resection or endoscopically guided biopsy; (II) availability of comprehensive MRI images; (III) absence of any prior history of neoadjuvant CRT along with the MRI scan. The criteria for exclusion were as follow: (I) suboptimal MRI image quality; (II) non-detectable tumor on the MRI imaging; (III) unresectable primary tumor or presence of metastatic diseases; (IV) tumor morphology consistent with mucinous cystadenoma. The participants were randomly allocated to TWIST and GRASP groups.

MRI acquisition

MRI scans were obtained using two systems: 3.0 T and 1.5 T MR, specifically the MAGNETOM Vida and MAGNETOM Aera, respectively, both manufactured by Siemens Healthineers in Erlangen, Germany. The GRASP acquisitions were exclusively executed utilizing the system of Vida, which was equipped with a 30-channel coil setup comprising of an 18-channel body coil and 12 channels derived from the spine coil. On the other hand, the TWIST acquisitions were solely conducted utilizing the Aera system, which was equipped with an 18-channel coil setup consisting of a 6-channel body coil and 12 channels derived from the spine coil. The individuals were positioned in a supine orientation with their heads placed first on the examination table. An enema was administered for bowel cleansing approximately 50 minutes prior to the assessment. In order to prevent possible bowel movement, the participants were given a 20 mg of intramuscular injection of scopolamine butyl bromide (Buscopan, Boehringer Ingelheim, Germany) half an hour prior to the imaging.

The standard MRI procedure comprised sagittal, axial (aligned perpendicularly to the rectum's long axis), oblique coronal T2-weighted images (T2WIs) without fat saturation, and DWI (aligned perpendicularly to the rectum's long axis). The perfusion protocol involved GRASP and TWIST sequences. Comprehensive protocol parameters for T2WI, DWI parameters, and perfusion sequences are provided in *Table 1*. The evaluation of the perfusion of GRASP or TWIST was performed following the intravenous administration of gadopentetate dimeglumine, which was adjusted according to the patient's body weight (0.1 mmol/kg BW, Dotarem; Guerbet, Paris, France) and delivered at a rate of 2 mL/s.

Image analysis

The manipulation of images was executed through the

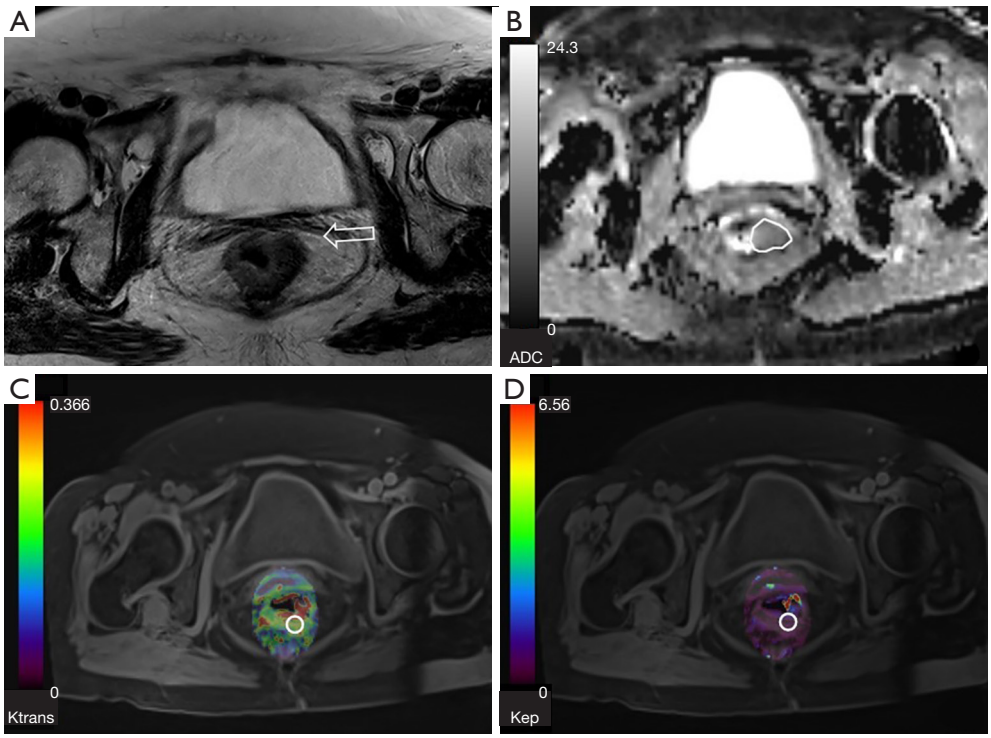

Figure 1 A 58-year-old man with median rectal cancer. (A) T2 weighted imaging, (B) apparent diffusion coefficient map (in units of 10^{-3} mm^2/s), (C) the Ktrans (in units of min^{-1}), and (D) Kep (in units of min^{-1}) of golden-angle radial sparse parallel, respectively. The white arrow points to the thickened tumor intestinal wall. The white circle refers to the tumor area of interest outlined by region of interest. Ktrans, influx forward volume transfer constant; Kep, rate constant.

utilization of a commercially obtainable program (Syngo. via VB30, MR Prostate, and MR Tissue4D; Siemens Healthineers, Shanghai, China). The quantitative pharmacokinetic model parameters were computed by means of the TOFTS model. These include the influx forward volume transfer constant, which is represented by the symbol Ktrans (min^{-1}), and the rate constant, which is commonly referred to as Kep (min^{-1}). The apparent diffusion coefficient (ADC) maps were generated utilizing a mono-exponential model depending on the Stejskal-Tanner equation (23). This model was employed to the DWI obtained at b-values of 50 and 1,000 s/mm^2.

The tumor location in individuals with RC was identified by two seasoned radiologists (MZ and TG) with six and ten years of experience in rectal imaging, respectively. Both of them had no information about the medical and pathological data regarding the patients and relied on the review of T2WI and DWI images. The Ktrans and Kep metrics were acquired through the delineation of the region of interest (ROI) on maps of perfusion, specifically targeting the top three layers of cancer lesions while taking care to exclude necrotic or cystic regions. The ultimate Ktrans and Kep values were obtained by computing the mean values achieved from delineating three distinct ROI levels (areas ≥1 cm^2) and subsequently calculating the average (*Figures 1,2*).

The ADC measurements were conducted by two radiologists who utilized a freehand technique to draw ROIs on the central cut of the tumor with a b-value of 1,000 s/mm^2. The ROIs were of enough dimension to cover the whole tumor region. The ROIs were transferred to the ADC maps while taking care to exclude regions of necrosis, vessels, and cysts as determined on T2WIs, in order to mitigate the bias. The last ADC values were computed by averaging the values acquired from three randomly selected ROIs located in distinct cancerous regions on three separate slices containing the cancer. The values of Ktrans, Kep, and ADC were subjected to averaging by the two radiologists for subsequent analysis (*Figures 1,2*).

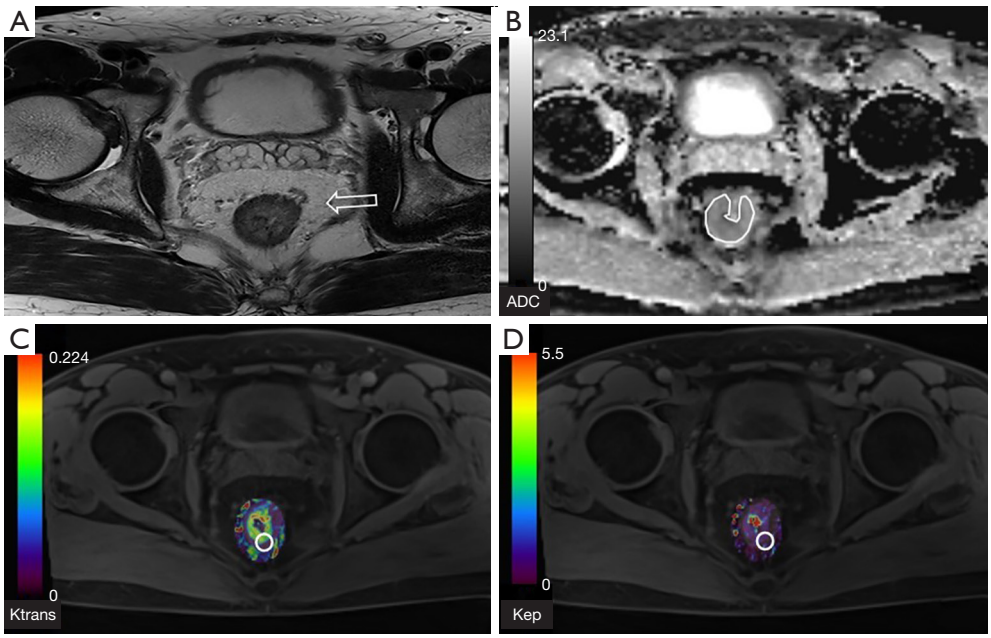

Figure 2 A 55-year-old man with median rectal cancer. (A) T2 weighted imaging, (B) apparent diffusion coefficient map (in units of 10^{-3} mm^2/s), (C) the Ktrans (in units of min^{-1}), and (D) Kep (in units of min^{-1}) of golden-angle radial sparse parallel, respectively. The white arrow points to the thickened tumor intestinal wall. The white circle refers to the tumor area of interest outlined by region of interest. Ktrans, influx forward volume transfer constant; Kep, rate constant.

Surgical histologic findings

To examine the tumors, we used a variety of instruments and procedures. Specifically, after surgical removal of the tumor, the tissue was treated with formalin and immersed in paraffin blocks. Segments of the blocks were cut at thickness of 4-micron and hematoxylin and eosin (H&E) was employed for staining to conduct histological analysis. The cancer differentiation degree was assessed by two expert pathologists who examined H&E-stained slides. The classification system used for differentiation was depended on the proportion of gland formation present in the tumor: cancers that were well differentiated exhibited glandular structures in excess of 95%, while moderately differentiated tumors displayed gland formation ranging from 50% to 95%. Poorly differentiated tumors were characterized by gland formation ranging from 5% to 50%, whereas undifferentiated tumors exhibited gland formation of less than 5% (24). In addition, immunohistochemical staining was performed to confirm the diagnosis and rule out other possible diagnoses (25).

Statistical analysis

We performed statistical analysis utilizing version 26 of SPSS (IBM Corporation, Armonk, NY, USA) and MedCalc (Version 16.8). The intraclass correlation coefficients (ICCs), based on the absolute agreement of a two-way mixed model, were computed to assess the agreement among Ktrans, Kep, and ADC values detected by the two radiologists for. We randomly selected 30% of cases (34 patients for the GRASP group and 27 patients for the TWIST group) for ICC calculation. The ICC agreement was classified into five distinct categories based on the magnitude of the coefficient: excellent (0.81–1.00), good (0.61–0.80), moderate (0.41–0.60), fair (0.21–0.4), and poor (ICC <0.2) (26). The mean values along with their corresponding standard deviations are reported for the ADC, Ktrans, and Kep parameters. The independent samples *t*-test and chi-squared test were used to compare medical data and quantitative parameters between the two groups (27). Our analyses focused on whether the amalgamation of diffusion and perfusion parameters could surpass the diagnostic accuracy of solely diffusion-based single-parameter evaluation. The study involved an analysis of various parameters, including ADC in combination with Ktrans, ADC in combination with Kep, and ADC alone. Receiver operating characteristic (ROC) curves were

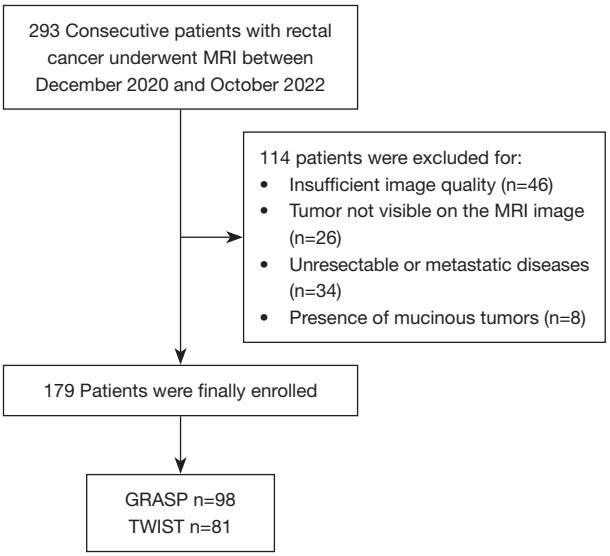

Figure 3 Flow diagram shows the inclusion and exclusion criteria for the study. GRASP, golden-angle radial sparse parallel; TWIST, view-sharing technique time-resolved angiography with stochastic trajectories.

Table 2 Clinical information of the two groups of patients

Characteristic	TWIST (n=81)	GRASP (n=98)	P value
Gender, n (%)			0.549
Male	65 (80.2)	75 (76.5)	
Female	16 (19.8)	23 (23.5)	
Age (years), mean ± SD	63.25±10.85	61.24±10.43	0.211
Tumor location, n (%)			0.938
High	27 (33.3)	32 (32.7)	
Medium	36 (44.4)	42 (42.9)	
Low	18 (22.2)	24 (24.5)	

The test level for the P value was 0.05. TWIST, time-resolved angiography with interleaved stochastic trajectories; GRASP, golden-angle radial sparse parallel.

utilized to pinpoint optimal cutoffs for each parameter, maximizing Youden's index (specificity + sensitivity – 1) (28). Comparison of the ROC curves was conducted employing the DeLong test. To control for type I error and adjust for multiple testing, we performed the Bonferroni correction on the significance level using a predefined formula (15,29):

$$p* = \alpha / m \quad [1]$$

where "$p*$" is the adjusted significance level, "α" is the critical P value, and "m" is the number of comparisons. The accuracy was detected as the sum of true positives and true negatives divided by the sum of all outcomes. The application of the Bonferroni correction resulted in the determination of an adjusted critical level of significance for pairwise testing, wherein a maximum of two hypotheses were considered. Specifically, P values less than 0.025 were utilized for comparisons of AUC. A two-sided P value of less than 0.05 was considered statistically significant.

Results

Patient characteristics

Typically, 293 patients diagnosed with non-mucinous rectal adenocarcinoma, depending on medical history and physical examination outcomes, were initially enrolled in this study. From this group, 114 patients were omitted owing to exclusion criteria: (I) image quality issues because of artifacts, preventing accurate ROI measurement (n=46); (II) tumor invisibility on MRI imaging (n=26); (III) presence of unresectable primary tumor or metastatic diseases (n=34); and (IV) presence of mucinous cystadenoma with low cell density and high ADC values (n=8). The final study group included 179 patients, of which 98 were examined using the GRASP method, and 81 underwent the TWIST procedure. The patient clinical information is shown in *Figure 3*. No statistically significant variation was detected in sex, age, and tumor location across the two groups (P=0.549, 0.211, 0.938) (*Table 2*).

Evaluation of the diagnostic accuracy of DCE-MRI and DWI

The study findings indicate that there was a significant variation in the ADC values between poorly differentiated RCs and well-moderately differentiated RCs in both groups (P<0.001). Moreover, Ktrans and Kep were significantly higher in poorly differentiated RCs across both groups (all P<0.001) (*Table 3*). The findings indicate that the ADC values exhibited superior precision in identifying poorly differentiated RC in the GRASP cohort, as compared to Ktrans (with a threshold value of 0.57 min^{-1}) or Kep (with a threshold of 0.93 min^{-1}). The cutoff value for the ADC values was determined to be 1.09×10^{-3} mm^2/s (*Table 4*).

Assessment of single-versus dual-parameter models

Our dual-parameter analysis exhibited that combining

Table 3 Results of differentiation between poorly differentiated and well-moderate differentiated rectal cancer

Study group	Well-moderate differentiated	Poor differentiated	P value
TWIST	n=62	n=19	
ADC-T (10^{-3} mm^2/s)	1.15±0.12	0.87±0.14	<0.001
Ktrans-T (min^{-1})	0.61±0.19	0.93±0.31	<0.001
Kep-T (min^{-1})	0.82±0.20	1.04±0.26	<0.001
GRASP	n=75	n=23	
ADC-G (10^{-3} mm^2/s)	1.12±0.14	0.90±0.10	<0.001
Ktrans-G (min^{-1})	0.63±0.19	0.83±0.17	<0.001
Kep-G (min^{-1})	0.84±0.25	1.05±0.19	<0.001

Data are mean ± standard deviation unless otherwise indicated. P values less than 0.05 were considered to indicate statistical significance. TWIST, time-resolved angiography with interleaved stochastic trajectories; ADC, apparent diffusion coefficient; Ktrans, influx forward volume transfer constant, Kep, rate constant; GRASP, golden-angle radial sparse parallel.

ADC threshold levels with either Ktrans or Kep depended on GRASP provided better diagnostic accuracy for poorly differentiated RC compared to single-parameter ADC-based evaluation (ADC with Ktrans *vs.* ADC, P=0.005; ADC with Kep *vs.* ADC, P=0.003). Although single-parameter assessment gave the best outcomes with ADC, combining ADC and TWIST-based perfusion cutoff levels did not provide a statistical advantage (*Table 4*). *Figure 4* illustrates how well-differentiated RCs can be more effectively distinguished when cutoff grades are based on ADC combined with perfusion parameters originated from GRASP, compared to ADC integrated with TWIST-derived perfusion parameters.

Interobserver agreement between the two groups

Both the TWIST and GRASP groups showed excellent interobserver agreement for Ktrans (ICC, 0.964; 95% CI: 0.899–0.985 and ICC, 0.918; 95% CI: 0.832–0.959, respectively), Kep (ICC, 0.901; 95% CI: 0.784–0.955 and ICC, 0.906; 95% CI: 0.768–0.957, respectively), and ADC (ICC, 0.905; 95% CI: 0.776–0.958 and ICC, 0.934; 95% CI: 0.144–0.983, respectively).

Discussion

Our outcomes reveal that combining the GRASP technique with established DWI in a dual-parameter approach yields a superior diagnostic capability for poorly differentiated RCs compared to the traditional single-parameter DWI-based evaluation. Notably, in contrast with well-moderately differentiated RCs, Ktrans and Kep were significantly greater in poorly differentiated RCs.

The differentiation grade of RCs is a factor influencing the prognosis (30). In our investigation, the ADC of poorly differentiated RCs was significantly reduced compared with well-moderately differentiated RCs (P<0.001), which was in line with prior research (31-34). Poorly differentiated cancer cells exhibit immature morphology and lack of function and therefore are typically higher in malignant potential compared to well or moderately differentiated tumors which are functionally and morphologically closer to the normal cell structure. Poorly differentiated cancer cells have a higher tendency to proliferate, infiltrate, and metastasize which makes their management more challenging. Furthermore, owing to their elevated proliferation rate, the ratio of nucleoplasm to cytoplasm rises, causing a reduction in extracellular space and impeding the unhindered movement of water molecules, culminating in diminished ADC values (35). The rise in the proportion of nucleus to cell density per unit volume resulted in a reduction of the distance of extracellular space and hindered the free diffusion of water molecules, ultimately causing a lessening in the ADC value (32). However, Tang *et al.* (36) reported no substantial variation in ADC values between diverse pathologic differentiation degrees in RC. This may be due to the different methodology employed to outline the ADC values.

Ktrans is a metric that quantifies the permeability of capillaries and the perfusion of blood in tissues, as well as the efficacy of contrast agents in traversing from blood vessels to the interstitial space. The existence of a greater

Table 4 Performance of models for prediction of poor differentiated rectal cancer

Performance of models	TWIST (n=81)	GRASP (n=98)
Performance of single-parameter models		
ADC (10^{-3} mm^2/s)		
Accuracy (%)	80 (n=65)	73 (n=72)
AUC	0.93±0.03	0.89±0.03
Ktrans (min^{-1})		
Accuracy (%)	84 (n=68)	54 (n=53)
AUC	0.81±0.06	0.77±0.05
Kep (min^{-1})		
Accuracy (%)	72 (n=58)	64 (n=63)
AUC	0.74±0.07	0.73±0.05
Performance of dual-parameter models		
ADC with Ktrans		
Accuracy (%)	86 (n=70)	90 (n=88)
AUC	0.93±0.04	0.97±0.02
ADC with Kep		
Accuracy (%)	93 (n=75)	93 (n=91)
AUC	0.93±0.03	0.97±0.02
P value		
ADC *vs.* ADC with Ktrans	0.955	0.005
ADC *vs.* ADC with Kep	0.981	0.003

AUC are presented as mean ± standard error. Perfusion parameters derived from TWIST and GRASP MRI study participant groups are shown. P<0.025 was considered to indicate statistical significance. TWIST, time-resolved angiography with interleaved stochastic trajectories; GRASP, golden-angle radial sparse parallel; ADC, apparent diffusion coefficient; AUC, area under the curve; Ktrans, influx forward volume transfer constant, Kep, rate constant.

number of capillaries in the presence of cancer results in an elevated Ktrans value (37). Similarly, an elevated Kep value indicates an increased blood supply to the vasculature. Consequently, an increase in Kep indicates a greater leakage of contrast medium. Moreover, Kep is exclusively influenced by the contrast concentration and fractional volumes within the Extravascular Extracellular Space (EES) of the tumor, which could potentially provide a more precise assessment of the cancer's capillary permeability (38). Our investigation discovered that Ktrans and Kep of poorly differentiated RCs were significantly greater than those of well-moderately differentiated RCs (P<0.001), which was along with earlier investigations (39,40). The tumors with higher degree of malignancy such as poorly differentiated RCs have impaired or increased capillary permeability which explains the results obtained in our and other studies (39).

Prior research has indicated a robust connection between quantitative parameters obtained from DCE-MRI and ADC values with medical and histological grade, response to neoadjuvant CRT, and predictive variables for diverse cancers (12-14). It is important to note, however, that conventional DCE-MRI has some limitations. Initially, it should be noted that the temporal resolution is estimated to be within the range of 5 to 18 seconds per phase. Subsequently, the acquisition process necessitates breath holds, which could potentially pose difficulties for certain patients and constrain the dynamic imaging's spatial and temporal resolution and volumetric coverage (41-45). This study utilized GRASP radial acquisition, which improved spatial and temporal resolutions over TWIST. According to previous studies (46,47), greater temporal resolution leads to enhanced precision of semi-quantitative and quantitative parameters acquired during DCE imaging. In addition to the findings mentioned above, it is worth noting that interobserver agreement was excellent for all measured parameters in both the TWIST and GRASP groups. These results indicate that the measurements obtained from the two different techniques were consistent and reliable, and the observers were consistent in interpreting the images.

As reported by Winkel *et al.* (15), GRASP can enhance the diagnostic efficacy of multiparametric MRI investigations of the prostate when both diffusion characteristics and perfusion characteristics are considered in the dual-parameter model. It was reported by Ao *et al.* (45) that the values of Ktrans and ADC served as separate markers for extramural venous invasion in RCs. Ma *et al.* (48) reported ADC value did not demonstrate statistical significance in identifying different kinds of RC. Based on the investigation by Oberholzer *et al.* (10), to evaluate cancer features connected with chemoradiation effectiveness prior to management start, MR perfusion may function as a complementary marker to the values of ADC. Our approach was inspired by the research performed by Winkel *et al.* (15), which used identical methods to evaluate prostate cancer with poor differentiation. However, we adopted this approach for the evaluation of RCs using GRASP instead of TWIST to enhance temporal resolution and reduce motion artifacts. The outcomes of this investigation indicate that the utilization of dual parameter

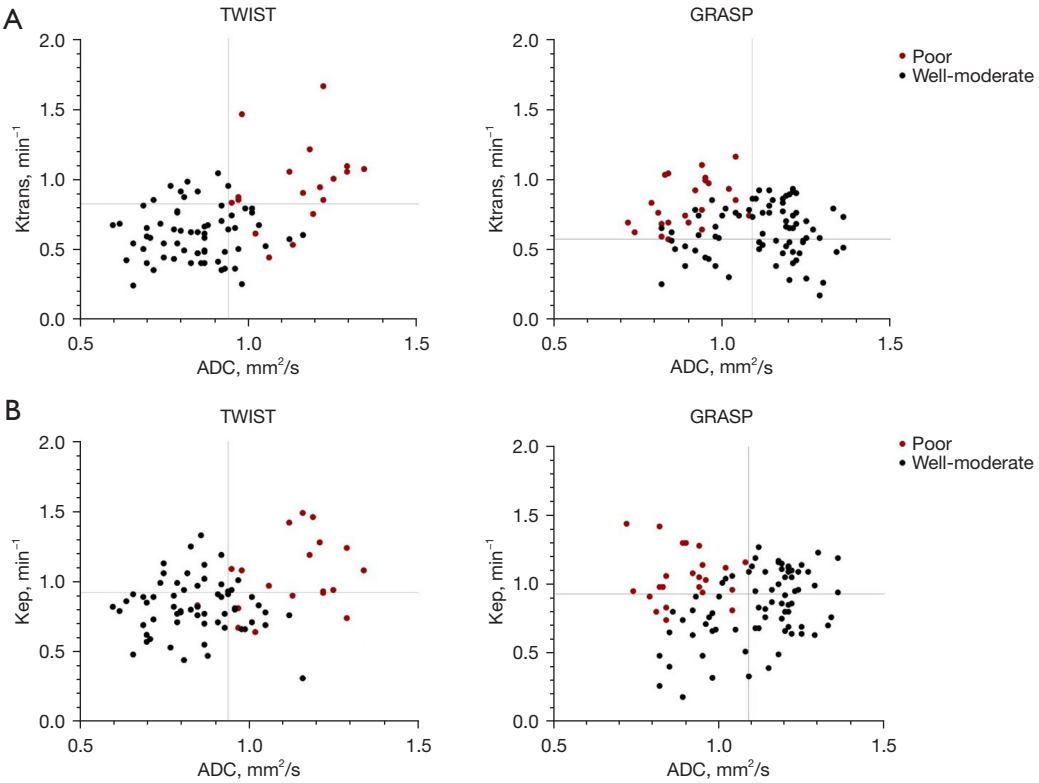

Figure 4 Quantitative assessment of combined diffusion MRI and dynamic contrast agent–enhanced MRI. Scatterplots display the data pairs of ADCs with Ktrans and ADC with Kep values. Horizontal and vertical lines represent the dual-parameter cutoff levels. TWIST, time-resolved angiography with interleaved stochastic trajectories; GRASP, golden-angle radial sparse parallel; ADC, apparent diffusion coefficient; Ktrans, influx forward volume transfer constant; Kep, rate constant.

examinations, which integrate values of ADC with either Ktrans or Kep obtained from the GRASP imaging technique, yielded a more accurate identification of poorly differentiated RCs compared to the single factor analysis of ADC. In terms of the accuracy of tumor detection, GRASP was the only procedure utilized to detect maps of perfusion. Therefore, it may be possible to hypothesize that the integrated elevated temporal and spatial resolution of the described acquisition methods helps in distinguishing between poorly differentiated and well-differentiated RCs.

Combining GRASP DCE-MRI with DWI has potential to improve RC diagnosis and treatment planning, however, there are some challenges that must be addressed before adopting this into clinical practice. It is necessary to standardize the imaging protocol across institutions to ensure consistent results. Large-scale multi-center studies are necessary to validate accuracy and establish generalizability. Well-trained radiologists and clinicians are also required to interpret complex imaging data.

Our study had limitations. Firstly, the investigation cohort exclusively comprised individuals diagnosed with RC confirmed through biopsy and surgical procedures. Subsequent investigations could encompass individuals with benign rectal injuries or those who underwent radiotherapy for RC to authenticate the investigation outcomes. Secondly, the study is a retrospective analysis conducted within a single institution. Further research is necessary to ascertain the repeatability of our findings in alternative healthcare establishments. Thirdly, there may be differences between the measurements of perfusion parameters between the TWIST and GRASP groups due to the different field strengths used in the MR scanners.

Conclusions

The outcomes of our investigation indicate that the utilization of parameters obtained from GRASP strategies leads to a significant enhancement in the diagnostic

accuracy of multiparametric MR scans for detecting RCs with poor differentiation. This improvement was achieved by integrating a dual-parameter model that incorporates both diffusion and perfusion features. Conversely, the TWIST perfusion parameters did not demonstrate this impact.

Acknowledgments

The authors thank Dr. Aamer Chughtai from Cleveland Clinic to help edit the language of the manuscript.
Funding: The study was supported by the National Natural Science Foundation of China (Nos. 81930046 and 81829003) and The Expert Workstation of Yunnan Province (Nos. 202105AF150037).

Footnote

Reporting Checklist: The authors have completed the STARD reporting checklist. Available at https://qims.amegroups.com/article/view/10.21037/qims-22-1244/rc

Conflicts of Interest: All authors have completed the ICMJE uniform disclosure form (available at https://qims.amegroups.com/article/view/10.21037/qims-22-1244/coif). FG reports that this research was funded by the National Natural Science Foundation of China (Nos. 81930046 and 81829003) and The Expert Workstation of Yunnan Province (No. 202105AF150037). YW holds the position of the head of the Research and Development Department at Sichuan Provincial People's Hospital. MC is an employee of Siemens Healthineers company. The other authors have no conflicts of interest to declare.

Ethical Statement: The authors are accountable for all aspects of the work in ensuring that questions related to the accuracy or integrity of any part of the work are appropriately investigated and resolved. The present study, which involved a retrospective analysis, received approval from the Institutional Review Board under the reference number Lun Audit (Research) No. 86 of 2021. Because of the retrospective nature of the investigation, the institutional review board waived the requirement for written informed consent. The study was conducted in compliance with the Declaration of Helsinki (as revised in 2013).

References

1. Asgeirsson T, Zhang S, Senagore AJ. Optimal follow-up to curative colon and rectal cancer surgery: how and for how long? Surg Oncol Clin N Am 2010;19:861-73.
2. Lee YC, Hsieh CC, Chuang JP. Prognostic significance of partial tumor regression after preoperative chemoradiotherapy for rectal cancer: a meta-analysis. Dis Colon Rectum 2013;56:1093-101.
3. Yang YS, Qiu YJ, Zheng GH, Gong HP, Ge YQ, Zhang YF, Feng F, Wang YT. High resolution MRI-based radiomic nomogram in predicting perineural invasion in rectal cancer. Cancer Imaging 2021;21:40.
4. Yang YS, Feng F, Qiu YJ, Zheng GH, Ge YQ, Wang YT. High-resolution MRI-based radiomics analysis to predict lymph node metastasis and tumor deposits respectively in rectal cancer. Abdom Radiol (NY) 2021;46:873-84.
5. Bown EJ, Lloyd GM, Boyle KM, Miller AS. Rectal cancer: prognostic indicators of long-term outcome in patients considered for surgery. Int J Colorectal Dis 2014;29:147-55.
6. DeVries AF, Kremser C, Hein PA, Griebel J, Krezcy A, Ofner D, Pfeiffer KP, Lukas P, Judmaier W. Tumor microcirculation and diffusion predict therapy outcome for primary rectal carcinoma. Int J Radiat Oncol Biol Phys 2003;56:958-65.
7. Engin G, Sharifov R, Güral Z, Sağam EK, Sağlam S, Balik E, Asoğu O, Yamaner S, Güllüoğu M, Kapran Y, Özel S. Can diffusion-weighted MRI determine complete responders after neoadjuvant chemoradiation for locally advanced rectal cancer? Diagn Interv Radiol 2012;18:574-81.
8. Lim JS, Kim D, Baek SE, Myoung S, Choi J, Shin SJ, Kim MJ, Kim NK, Suh J, Kim KW, Keum KC. Perfusion MRI for the prediction of treatment response after preoperative chemoradiotherapy in locally advanced rectal cancer. Eur Radiol 2012;22:1693-700.
9. Nougaret S, Fujii S, Addley HC, Bibeau F, Pandey H, Mikhael H, Reinhold C, Azria D, Rouanet P, Gallix B. Neoadjuvant chemotherapy evaluation by MRI volumetry

in rectal cancer followed by chemoradiation and total mesorectal excision: Initial experience. J Magn Reson Imaging 2013;38:726-32.
10. Oberholzer K, Menig M, Pohlmann A, Junginger T, Heintz A, Kreft A, Hansen T, Schneider A, Lollert A, Schmidberger H, Christoph D. Rectal cancer: assessment of response to neoadjuvant chemoradiation by dynamic contrast-enhanced MRI. J Magn Reson Imaging 2013;38:119-26.
11. Patel UB, Blomqvist LK, Taylor F, George C, Guthrie A, Bees N, Brown G. MRI after treatment of locally advanced rectal cancer: how to report tumor response--the MERCURY experience. AJR Am J Roentgenol 2012;199:W486-95.
12. Delli Pizzi A, Mastrodicasa D, Marchioni M, Primiceri G, Di Fabio F, Cianci R, Seccia B, Sessa B, Mincuzzi E, Romanelli M, Castellan P, Castellucci R, Colasante A, Schips L, Basilico R, Caulo M. Bladder cancer: do we need contrast injection for MRI assessment of muscle invasion? A prospective multi-reader VI-RADS approach. Eur Radiol 2021;31:3874-83.
13. Nerad E, Delli Pizzi A, Lambregts DMJ, Maas M, Wadhwani S, Bakers FCH, van den Bosch HCM, Beets-Tan RGH, Lahaye MJ. The Apparent Diffusion Coefficient (ADC) is a useful biomarker in predicting metastatic colon cancer using the ADC-value of the primary tumor. PLoS One 2019;14:e0211830.
14. Gürses B, Böge M, Altınmakas E, Balık E. Multiparametric MRI in rectal cancer. Diagn Interv Radiol 2019;25:175-82.
15. Winkel DJ, Heye TJ, Benz MR, Glessgen CG, Wetterauer C, Bubendorf L, Block TK, Boll DT. Compressed Sensing Radial Sampling MRI of Prostate Perfusion: Utility for Detection of Prostate Cancer. Radiology 2019;290:702-8.
16. Davenport MS, Heye T, Dale BM, Horvath JJ, Breault SR, Feuerlein S, Bashir MR, Boll DT, Merkle EM. Inter- and intra-rater reproducibility of quantitative dynamic contrast enhanced MRI using TWIST perfusion data in a uterine fibroid model. J Magn Reson Imaging 2013;38:329-35.
17. Attenberger UI, Liu J, Riffel P, Budjan J, Grimm R, Block KT, Schoenberg SO, Wang X, Hausmann D. Quantitative Perfusion Analysis of the Rectum Using Golden-Angle Radial Sparse Parallel Magnetic Resonance Imaging: Initial Experience and Comparison to Time-Resolved Angiography With Interleaved Stochastic Trajectories. Invest Radiol 2017;52:715-24.
18. Riffel P, Zoellner FG, Budjan J, Grimm R, Block TK, Schoenberg SO, Hausmann D. "One-Stop Shop": Free-Breathing Dynamic Contrast-Enhanced Magnetic Resonance Imaging of the Kidney Using Iterative Reconstruction and Continuous Golden-Angle Radial Sampling. Invest Radiol 2016;51:714-9.
19. Li Y, Xia C, Peng W, Gao Y, Hu S, Zhang K, Zhao F, Benkert T, Zhou X, Zhang H, Li Z. Dynamic contrast-enhanced MR imaging of rectal cancer using a golden-angle radial stack-of-stars VIBE sequence: comparison with conventional contrast-enhanced 3D VIBE sequence. Abdom Radiol (NY) 2020;45:322-31.
20. Prampolini F, Taschini S, Pecchi A, Sani F, Spallanzani A, Gelsomino F, Kaleci S, Torricelli P. Magnetic resonance imaging performed before and after preoperative chemoradiotherapy in rectal cancer: predictive factors of recurrence and prognostic significance of MR-detected extramural venous invasion. Abdom Radiol (NY) 2020;45:2941-9.
21. Wu LF, Rao SX, Xu PJ, Yang L, Chen CZ, Liu H, Huang JF, Fu CX, Halim A, Zeng MS. Pre-TACE kurtosis of ADC(total) derived from histogram analysis for diffusion-weighted imaging is the best independent predictor of prognosis in hepatocellular carcinoma. Eur Radiol 2019;29:213-23.
22. Granata V, Grassi R, Fusco R, Izzo F, Brunese L, Delrio P, Avallone A, Pecori B, Petrillo A. Current status on response to treatment in locally advanced rectal cancer: what the radiologist should know. Eur Rev Med Pharmacol Sci 2020;24:12050-62.
23. Le Bihan D, Breton E, Lallemand D, Grenier P, Cabanis E, Laval-Jeantet M. MR imaging of intravoxel incoherent motions: application to diffusion and perfusion in neurologic disorders. Radiology 1986;161:401-7.
24. Nagtegaal ID, Odze RD, Klimstra D, Paradis V, Rugge M, Schirmacher P, Washington KM, Carneiro F, Cree IA; WHO Classification of Tumours Editorial Board. The 2019 WHO classification of tumours of the digestive system. Histopathology 2020;76:182-8.
25. Maguire A, Sheahan K. Controversies in the pathological assessment of colorectal cancer. World J Gastroenterol 2014;20:9850-61.
26. Peng Y, Li Z, Tang H, Wang Y, Hu X, Shen Y, Hu D. Comparison of reduced field-of-view diffusion-weighted imaging (DWI) and conventional DWI techniques in the assessment of rectal carcinoma at 3.0T: Image quality and histological T staging. J Magn Reson Imaging 2018;47:967-75.
27. Yuan Y, Chen XL, Li ZL, Chen GW, Liu H, Liu YS, Pang

MH, Liu SY, Pu H, Li H. The application of apparent diffusion coefficients derived from intratumoral and peritumoral zones for assessing pathologic prognostic factors in rectal cancer. Eur Radiol 2022;32:5106-18.
28. Youden WJ. Index for rating diagnostic tests. Cancer 1950;3:32-5.
29. Sedgwick P. Multiple hypothesis testing and Bonferroni's correction. BMJ 2014;349:g6284.
30. Zhu L, Pan Z, Ma Q, Yang W, Shi H, Fu C, Yan X, Du L, Yan F, Zhang H. Diffusion Kurtosis Imaging Study of Rectal Adenocarcinoma Associated with Histopathologic Prognostic Factors: Preliminary Findings. Radiology 2017;284:66-76.
31. Akashi M, Nakahusa Y, Yakabe T, Egashira Y, Koga Y, Sumi K, Noshiro H, Irie H, Tokunaga O, Miyazaki K. Assessment of aggressiveness of rectal cancer using 3-T MRI: correlation between the apparent diffusion coefficient as a potential imaging biomarker and histologic prognostic factors. Acta Radiol 2014;55:524-31.
32. Curvo-Semedo L, Lambregts DM, Maas M, Beets GL, Caseiro-Alves F, Beets-Tan RG. Diffusion-weighted MRI in rectal cancer: apparent diffusion coefficient as a potential noninvasive marker of tumor aggressiveness. J Magn Reson Imaging 2012;35:1365-71.
33. Cho EY, Kim SH, Yoon JH, Lee Y, Lim YJ, Kim SJ, Baek HJ, Eun CK. Apparent diffusion coefficient for discriminating metastatic from non-metastatic lymph nodes in primary rectal cancer. Eur J Radiol 2013;82:e662-8.
34. Holdsworth SJ, Yeom K, Skare S, Gentles AJ, Barnes PD, Bammer R. Clinical application of readout-segmented-echo-planar imaging for diffusion-weighted imaging in pediatric brain. AJNR Am J Neuroradiol 2011;32:1274-9.
35. Jögi A, Vaapil M, Johansson M, Påhlman S. Cancer cell differentiation heterogeneity and aggressive behavior in solid tumors. Ups J Med Sci 2012;117:217-24.
36. Tang C, Lin MB, Xu JL, Zhang LH, Zuo XM, Zhang ZS, Liu MX, Xu JM. Are ADC values of readout-segmented echo-planar diffusion-weighted imaging (RESOLVE) correlated with pathological prognostic factors in rectal adenocarcinoma? World J Surg Oncol 2018;16:138.
37. Zhu Y, Zhou Y, Zhang W, Xue L, Li Y, Jiang J, Zhong Y, Wang S, Jiang L. Value of quantitative dynamic contrast-enhanced and diffusion-weighted magnetic resonance imaging in predicting extramural venous invasion in locally advanced gastric cancer and prognostic significance. Quant Imaging Med Surg 2021;11:328-40.
38. Koo HR, Cho N, Song IC, Kim H, Chang JM, Yi A, Yun BL, Moon WK. Correlation of perfusion parameters on dynamic contrast-enhanced MRI with prognostic factors and subtypes of breast cancers. J Magn Reson Imaging 2012;36:145-51.
39. Li M, Xu X, Xia K, Jiang H, Jiang J, Sun J, Lu Z. Comparison of Diagnostic Performance between Perfusion-Related Intravoxel Incoherent Motion DWI and Dynamic Contrast-Enhanced MRI in Rectal Cancer. Comput Math Methods Med 2021;2021:5095940.
40. Shen FU, Lu J, Chen L, Wang Z, Chen Y. Diagnostic value of dynamic contrast-enhanced magnetic resonance imaging in rectal cancer and its correlation with tumor differentiation. Mol Clin Oncol 2016;4:500-6.
41. Dijkhoff RAP, Maas M, Martens MH, Papanikolaou N, Lambregts DMJ, Beets GL, Beets-Tan RGH. Correlation between quantitative and semiquantitative parameters in DCE-MRI with a blood pool agent in rectal cancer: can semiquantitative parameters be used as a surrogate for quantitative parameters? Abdom Radiol (NY) 2017;42:1342-9.
42. Hötker AM, Tarlinton L, Mazaheri Y, Woo KM, Gönen M, Saltz LB, Goodman KA, Garcia-Aguilar J, Gollub MJ. Multiparametric MRI in the assessment of response of rectal cancer to neoadjuvant chemoradiotherapy: A comparison of morphological, volumetric and functional MRI parameters. Eur Radiol 2016;26:4303-12.
43. Zhang XM, Yu D, Zhang HL, Dai Y, Bi D, Liu Z, Prince MR, Li C. 3D dynamic contrast-enhanced MRI of rectal carcinoma at 3T: correlation with microvascular density and vascular endothelial growth factor markers of tumor angiogenesis. J Magn Reson Imaging 2008;27:1309-16.
44. Chen L, Zeng X, Ji B, Liu D, Wang J, Zhang J, Feng L. Improving dynamic contrast-enhanced MRI of the lung using motion-weighted sparse reconstruction: Initial experiences in patients. Magn Reson Imaging 2020;68:36-44.
45. Ao W, Zhang X, Yao X, Zhu X, Deng S, Feng J. Preoperative prediction of extramural venous invasion in rectal cancer by dynamic contrast-enhanced and diffusion weighted MRI: a preliminary study. BMC Med Imaging 2022;22:78.
46. Michaely HJ, Sourbron SP, Buettner C, Lodemann KP, Reiser MF, Schoenberg SO. Temporal constraints in renal perfusion imaging with a 2-compartment model. Invest Radiol 2008;43:120-8.
47. Othman AE, Falkner F, Weiss J, Kruck S, Grimm R, Martirosian P, Nikolaou K, Notohamiprodjo M. Effect

of Temporal Resolution on Diagnostic Performance of Dynamic Contrast-Enhanced Magnetic Resonance Imaging of the Prostate. Invest Radiol 2016;51:290-6.
48. Ma L, Lian S, Liu H, Meng T, Zeng W, Zhong R, Zhong L, Xie C. Diagnostic performance of synthetic magnetic resonance imaging in the prognostic evaluation of rectal cancer. Quant Imaging Med Surg 2022;12:3580-91.

Cite this article as: Zhou M, Huang H, Fan Y, Chen M, Wang Y, Gao F. Golden-angle radial sparse parallel magnetic resonance imaging of rectal perfusion: utility in the diagnosis of poorly differentiated rectal cancer. Quant Imaging Med Surg 2023;13(8):4826-4838. doi: 10.21037/qims-22-1244

